Journal of Applied Mechanics Vol.11, pp.389-398 (August 2008) JSCE

Modeling of Microstructural Evolution to Simulate Undrained Shear Strength Variation of Kaolin Clay

N.H. Minh *, M. Oda**, K. Suzuki *** and L.C. Kurukulasuriya ****

* Doctoral student, Dept. of Civil & Environ. Eng., Saitama University (255 Shimo-okubo, Sakura-ku, Saitama 338-8570)
** Professor, Dept. of Civil & Environ. Eng., Saitama University (255 Shimo-okubo, Sakura-ku, Saitama 338-8570)
*** Assoc. Professor, Dept. of Civil & Environ. Eng., Saitama University (255 Shimo-okubo, Sakura-ku, Saitama 338-8570)
**** Senior Lecturer, Dept. of Civil Eng. University of Peradeniya (Peradeniya, 20400, Sri Lanka)

The microstructure of soils is, in general, anisotropic in both the "inherent" and "induced" senses described by Casagrande and Carillo[1], which yield anisotropic responses for both strength and plastic deformation. The undrained shear strength of clayey soils, for example, changes greatly depending on the inclination angle θ of the loading direction with respect to the consolidation plane. In the present study on constitutive modeling, a tensorial quantity called the fabric tensor is incorporated into the classical plasticity framework to simulate the effects of microstructure on the variation of undrained shear strength of Kaolin clay. The effects of inherent and induced anisotropies are considered in terms of an evolution rule of the fabric tensor. It is shown that the proposed model can simulate well the variation of undrained shear strength observed in plane strain experiments of normally consolidated Kaolin clay by Kurukulasuriya[2].

Key Words: *inherent anisotropy, induced anisotropy, fabric tensor, undrained shear strength*

1. Introduction

Studies on the microstructure of clays (e.g., Kazama[3]; Kurukulasuriya[2]) have shown that platy clay minerals tend to align their faces perpendicular to the direction of consolidation so that the microstructure of the soil skeleton becomes anisotropic. Anisotropy in soils is commonly classified into two categories, i.e., inherent and induced anisotropies (Casagrande and Carillo[1]). The former is concerned with the anisotropy developed during the sedimentation process under gravity, while the latter is mainly concerned with the anisotropy arising from the evolution of microstructure associated with plastic deformation after sedimentation. From a micro-structural point of view, however, both are formed by preferred orientation of constituent elements, such as particles, voids, and contact surfaces (Oda[4]). Furthermore, Satake[5] and Oda et al.[6] have shown that the preferred orientation of these elements can be quantified by introducing a tensorial quantity called the fabric tensor. The structural anisotropy yields anisotropic responses in both the strength and plastic deformation of soils. For example, the undrained shear strength c_u, which plays a dominant role in stability analyses of soil foundations, changes considerably depending on the inclination angle θ of the loading direction against the consolidation plane (normal to the consolidation axis) (e.g., Duncan and Seed[7,8]; Kazama[3]; Kurukulasuriya[2]). It is of particular importance that such a relation between c_u and θ can be different for different soils. Duncan and Seed[8], for example, showed that three different patterns, each of which was individually found in undrained triaxial tests on natural soils one-dimensionally consolidated in the field (Fig. 1). Importantly, such differences exist even though all soils were one-dimensionally consolidated under a similar condition. How can we explain this interesting observation? As far as we know, no valid explanation has yet been presented. However, the initial microstructure and its subsequent evolution might be closely related to the formation of such different patterns.

In a previous study on the modeling of inherent anisotropy (Minh et al.[9]), the microstructure of Kaolin clay is taken into account in terms of a constant fabric tensor. However, the modeling of inherent anisotropy, which leads to a monotonic increase of undrained shear strength with θ, is not sufficient to simulate successfully the approximately bilinear relationship between c_u and θ as being plotted in Fig. 2 by Kurukulasuriya[2] for Kaolin clay. In this study, the modeling of microstructural anisotropy is extended such that the effects of both inherent and induced anisotropies can be taken into account with the introduction of an evolution rule of the fabric tensor during the shearing process as well as its stationary values at the initial and ultimate conditions. The simulated results using the proposed constitutive model agree well with the experimental data by Kurukulasuriya[2] for normally consolidated Kaolin clay. Furthermore, the study provides an approach to connect results from micromechanics research field with conventional continuum modeling.

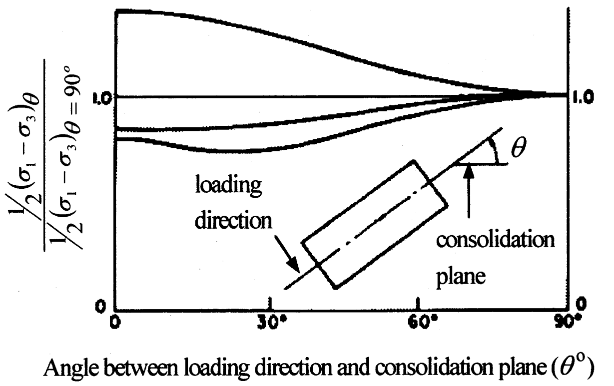

Fig. 1 Variations of strength using UU tests (Duncan and Seed[8])

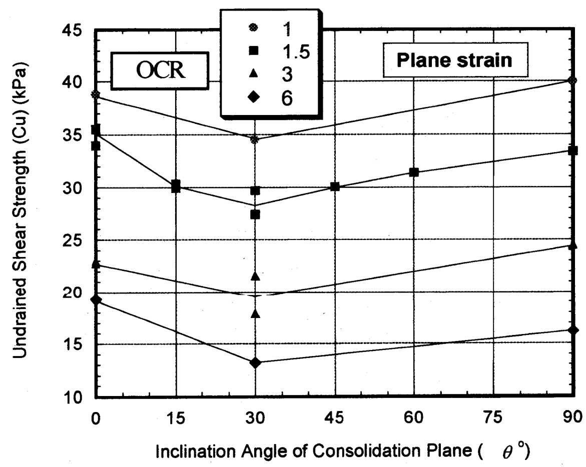

Fig. 2 Variations of undrained shear strength of Kaolin clay (Kurukulasuriya[2])

2. Plane Strain Tests of Kaolin Clay

In order to analyze in detail the undrained shear strength anisotropy of clay, we frequently refer to a series of plane strain tests carried out by Kurukulasuriya[2]. Kaolin clay, the material used in the experiments, was prepared under a K_0 – consolidation process with a maximum vertical pressure of 150 kPa. After K_0 – consolidation was completed, parallelepiped samples (5 × 10 × 12.5 cm) for plane strain tests were made from the material such that the sample axes were inclined at different angles θ to the consolidation (horizontal) plane. The sample was next placed in a plane strain test apparatus and consolidated under an isotropic confining pressure p_0. After isotropic consolidation, the sample was sheared under the undrained plane strain condition to determine the undrained shear strength (= maximum shear stresses at failure). There are two points worth noting here. 1) Experimental evidence suggests that the anisotropic microstructure developed during the K_0 – consolidation process is preserved, to a certain extent, throughout the isotropic consolidation. 2) The isotropic consolidation excludes the effects of the anisotropic initial stress condition on the variation of undrained shear strength (see Duncan and Seed[8]). Accordingly, the undrained shear strength anisotropy, if it exists, can only develop from the anisotropic microstructure of Kaolin clay developed during K_0 – consolidation. Figure 2 describes the variation of the undrained shear strength of Kaolin clay as a function of the inclination angle θ for the plane strain testing condition. The undrained shear strength varies in a similar manner with a minimum around θ = 30°, irrespective of the OCR (=150/p_0) values.

3. Constitutive Modeling

3.1 Fabric Tensor and the Evolution of Fabric Tensor

Particles in soils are seldom spherical in shape, anisotropy is consequently produced by the preferred orientation of these non-spherical particles. In the case of Kaolin minerals, particles are platy so that the microstructures can conveniently be defined by considering the spatial distribution of unit vectors **n** normal to their major planes. The fabric tensor F_{ij} can be given as:

$$F_{ij} = \int_{\Omega} n_i n_j E(\mathbf{n}) d\Omega \tag{1}$$

where Ω is a solid angle equal to a surface of a unit sphere, n_i (i = 1,2,3) are X_i - components of a unit normal vector **n**, and E(**n**) is a density function such that $E(\mathbf{n})d\Omega$ corresponds to the rate of unit vectors oriented within a small solid angle $d\Omega$. By definition, E(**n**) must satisfy $\int_{\Omega} E(\mathbf{n}) d\Omega = 1$, leading to the trace of the fabric tensor F_{ii} being equal to 1. Let us assume that the microstructure of soils is axial-symmetric with a symmetry axis parallel to the consolidation direction (or vertical direction). That is, the microstructure is anisotropic on the vertical plane, including the consolidation direction, whereas it is isotropic on the horizontal plane perpendicular to the consolidation direction. This assumption is consistent with the microscopic observations on the microstructure of natural clay by Kazama[3] and of sand by Oda[4]. If this is the case, the fabric tensor of Eq. (1) can further be simplified. Let x_α (α =1,2,3) be a local coordinate system such that x_1 is the consolidation direction, and x_2 and x_3 are on the plane perpendicular to x_1. Since the microstructure is axially symmetric with a symmetry axis parallel to x_1, it agrees with the major principal axis of fabric tensor $F_{\alpha\beta}$. (Note that the subscripts α and β refer to the principle axes x_α (α =1,2,3), whereas the subscripts i and j in Eq. (1) refer to global coordination axes X_i (i = 1,2,3) defined later.) In this case, F_{11}, F_{22} = F_{33} are the principal values. Let r be a ratio of F_{11} to F_{22} (= F_{33}), then we have:

$$F_{11} = rF_{22}, F_{22} = F_{33} \tag{2}$$

where r is hereinafter referred to as the degree of anisotropy. Since the trace of the fabric tensor is equal to 1, we have the following expression:

$$\begin{aligned} F_{\alpha\beta} &= (F_{11}, F_{22}, F_{33}, F_{12}, F_{23}, F_{13}) \\ &= (r/(2+r), 1/(2+r), 1/(2+r), 0,0,0) \end{aligned} \tag{3}$$

If the microstructure is isotropic, the degree of anisotropy r is set to 1 with the following isotropic tensor:

$$\begin{aligned} F_{\alpha\beta} &= (F_{11}, F_{22}, F_{33}, F_{12}, F_{23}, F_{13}) \\ &= (1/3, 1/3, 1/3, 0,0,0) \end{aligned} \tag{4}$$

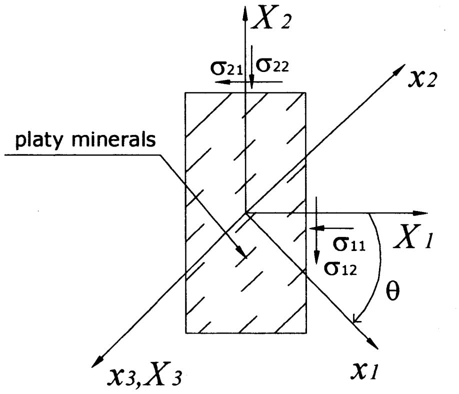

Fig. 3 Principal axes x_α (α=1,2,3) of the fabric tensor and X_i (i =1,2,3) axes of the global coordination system

A global coordination system X_i (i = 1,2,3) is introduced such that X_2 is parallel to the vertical plane, and X_1 and X_3 are on the horizontal plane (Fig. 3). In the following numerical simulations, the major compression direction is always parallel to X_2. In addition, θ is defined as the inclination angle between the global horizontal axis X_1 and the major principal axis x_1 of the fabric tensor. (Note that this definition of θ is equivalent to that in Fig. 1.) Note also that the components of Eqs. (3) and (4) were calculated with respect to the principal axes x_α of the fabric tensor. The components of the fabric tensor with respect to the global axes X_i (i = 1,2,3) could, if necessary, be calculated using the coordinate transformation rule of the tensor.

If only the effects of inherent anisotropy are taken into account, the fabric tensor is assumed to be constant through out the shearing process. In this case, since the fabric tensor at the initial and ultimate conditions are the same, its value could be calculated from the stress conditions measured at the ultimate condition from two experiments with different values of θ (see Minh et al.[9]). However, for induced anisotropy, the distribution of the contact normals, which reflects the microstructure of materials, changes its value in accordance with the application of the loading increments. Consequently, it is necessary to define an equation to formularize the evolution of the contact normals during the shearing process. Note that the induced anisotropy is different with the stress-induced anisotropy phenomenon. Ohta and Nishihara[10], for example, described stress-induced anisotropy as: "an apparent anisotropy caused by the anisotropic initial stress state". The stress-induced anisotropy requires mechanical soil properties to be isotropic in their nature. On the other hand, the mechanical soil properties in this model, e.g. the critical parameter M or plastic modulus, vary depending on θ value.

The states of the fabric tensor at the initial and ultimate conditions must be also quantified so as the fabric tensor at any other state in between these two extremes could be determined using the aforementioned evolution rule of the fabric tensor. For example, the fabric tensor at step n could be calculated as follows:

$$F_{ij}^{n} = (F_{ij}^{ini} + \sum_{k=1,n-1} dF_{ij}^{k}) / F_{mm}^{n} \tag{5}$$

where $F_{ij}^{ini}, dF_{ij}^{k}$ are the initial fabric tensor and the increment of fabric tensor at step k, respectively. It is noted that in Eq. (5), all the components of the newly updated fabric tensor F_{ij}^{n} are normalized with the trace of itself F_{mm}^{n} in order to maintain the condition of F_{ii} = 1 from the definition of the fabric tensor in Eq. (1). According to Oda[11], the concentration of the contact normals is found to depend on the increment of deviatoric stress tensor, ds_{ij} (where $s_{ij} = \sigma'_{ij} - p\delta_{ij}$). Furthermore, there exists a limitation for the value of $\sqrt{J_{2D}^{F}}$ (where J_{2D}^{F} is the second deviatoric invariant of the fabric tensor), which represents a certain saturated value for the concentration of the contact normals. Based on this observation, it is assumed that any state of the fabric tensor, including the initial and ultimate conditions, could be defined in terms of $\sqrt{J_{2D}^{F}}$. The value of $\sqrt{J_{2D}^{F}}$ at ultimate condition, $(\sqrt{J_{2D}^{F}})_{ult}$, and consequently, $(F_{ij})_{ult}$, could be calculated from the measured stress values at the critical state. Applying the calculation procedure described by Minh et al.[9] for the testing data of Kaolin clay by Kurukulasuriya[2], we could obtain the degree of anisotropy r_{ult} = 1.06 at the ultimate condition, which then could be used to calculate $(F_{ij})_{ult}$ and consequently, $(\sqrt{J_{2D}^{F}})_{ult} = 0.01132$. Details on the calculation of r_{ult} are described later in this paper. On the other hand, the fabric tensor at the beginning of the shearing process, $(F_{ij})_{ini}$, which represents the effects of the inherent anisotropy of Kaolin clay, could be determined by conducting the simulation of the K_0– consolidation process. For simplicity, however, we assume here the following relation on a tentative basis; i.e., $\left(\sqrt{J_{2D}^{F}}\right)_{ini} = 0.8\left(\sqrt{J_{2D}^{F}}\right)_{ult}$. This is equivalent to the assumption that when K_0 – consolidation is completed, the microstructural anisotropy is given by $r_{ult} = 1.048$, and as the result of the fabric evolution, r consequently reaches 1.06 at the end of the shearing process. Since the concentration of the contact normals is related to ds_{ij}, dF_{ij} can be formulated in the following form:

$$dF_{ij} = kds_{ij} \tag{6}$$

where k is a constant of proportionality expressed as:

$$k = k\left(\psi, (J_{2D}^F)_{ult}, J_{2D}^F\right) \tag{7}$$

where ψ is the angle between the major principal axes of F_{ij} and ds_{ij}. It is reasonable to think that large fabric change is likely to occur when the compressive loading is applied parallel to the direction of the minimum concentration of the contact normal at the current state. As the result, k should be an increasing function of ψ with a maximum at $\psi = 90°$. That is, the fabric change occurs faster in the case of $\theta = 0°$ than that in the case of $\theta = 90°$ in the early stage of deformation at least. Based on the above consideration, we assume the following function:

$$k = a\left(1.2e^{b|\sin\psi|} - 1\right)\left((J_{2D}^F)_{ult} - J_{2D}^F\right) \tag{8}$$

where a is a constant serving as a scaling factor, and b is an another parameter to control how rapidly k lowers its value with decreasing ψ. With the introduction of Eqs. (6) and (8) as well as the values of $(F_{ij})_{ini}$ and $(F_{ij})_{ult}$, the evolution of the fabric tensor from the beginning of the test until the ultimate condition is completely defined.

It should be noted that Eq. (6) and Eq. (7) were firstly introduced by Oda[11] based on microscopic observation of granular material behavior. In this study, it is an attempt to apply the same results for Kaolin clay. Since we have no clear experimental evidence on the microstructural evolution of Kaolin clay, the direct application of Eq. (6) and Eq. (7) for Kaolin clay in this case may involve some uncertainties. However, we accept this assumption in order to seek for an alternative modeling solution. As it is turn out later, the application of fabric tensor and fabric change for Kaolin clay actually leads to good prediction of undrained shear strength variation of Kaolin clay. This phenomenon, otherwise, could not be simulated using conventional plasticity constitutive models.

3.2 Modified Stress

In order to account for the microstructure of granular materials, Tobita[12] and Oda[11] introduced a modified stress tensor T_{ij} in terms of the fabric tensor F_{ij} and the conventional stress tensor σ_{ij}. Figure 4a shows three orthogonal planes having unit area, hereinafter, referred to as the x_α - plane, the normal directions of which are parallel to the principal axes x_α of the fabric tensor. The hatched and hollow particles show two groups of particles, the centers of which are located inside and outside, respectively, of a unit cube enclosed by three sets of x_α - planes.

Any force applied to these planes would be transferred through contact areas between the particles belonging to these two groups. More importantly, sliding and rolling of particles (plastic deformation) occurs at contacts according to conditions satisfied by contact forces. Accordingly, it appears reasonable to think that in order to deal with the plastic behavior of granular soils, stress can be defined with respect to the contact surfaces rather than the unit area of the x_α - planes in the definition of conventional stress.

Particles are so small that many contact areas are associated with each orthogonal unit plane. The contact areas associated with the x_α - planes are projected on the x_α - planes and then summed to obtain the contact surface areas c_α (α =1,2,3). For reasons that will be clarified later, c_α (α =1,2,3) are proportionally enlarged such that the summation of three enlarged contact areas C_α ($C_\alpha = a\,c_\alpha$) is equal to 3 (i.e., $C_1 + C_2 + C_3 = 3$). Note that C_α (α =1,2,3) can reflect the anisotropic distribution of the contact areas through which the applied forces are actually transmitted through the assembly. The modified stress is then introduced as the imaginary stress $T_{\alpha\beta}$ acting on the enlarged contact surfaces C_α (α=1,2,3) (Fig. 4b). The modified stress tensor is defined for such a condition that the integration of conventional stress $\sigma_{\alpha\beta}$ over the x_α - planes must equal the integration of modified stress $T_{\alpha\beta}$ over the x_α - surfaces. This leads to the following relations:

$$\begin{pmatrix} T_{11} & T_{12} & T_{13} \\ & T_{22} & T_{23} \\ Sym. & & T_{33} \end{pmatrix} = \begin{pmatrix} 1/C_1 & 0 & 0 \\ & 1/C_2 & 0 \\ Sym. & & 1/C_3 \end{pmatrix} \begin{pmatrix} \sigma_{11} & \sigma_{12} & \sigma_{13} \\ & \sigma_{22} & \sigma_{23} \\ Sym. & & \sigma_{33} \end{pmatrix} \tag{9}$$

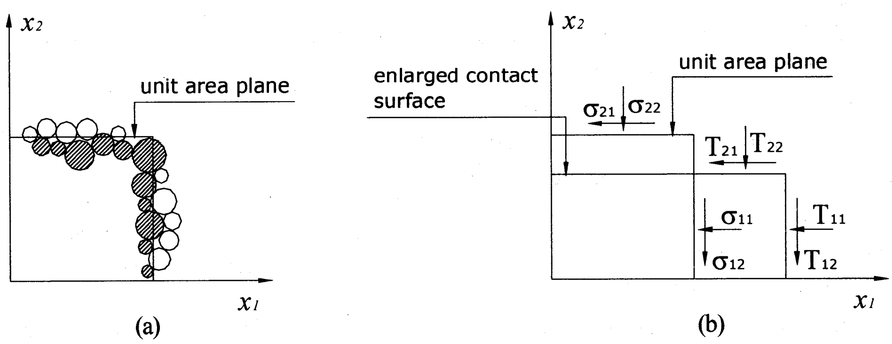

Fig. 4 (a) Orthogonal planes cutting through a particle assembly (b) conventional stress tensor, $\sigma_{\alpha\beta}$, acting on a unit plane and modified stress tensor, $T_{\alpha\beta}$, acting on enlarged contact surfaces

Equation (9) is given with respect to the principal axes x_α (α =1,2,3) of the microstructure. Referring to the global axes X_i (i =1,2,3), we can easily generalize Eq. (9) as:

$$T_{ij} = C_{ik}^{-1}\sigma_{kj} \quad \text{or} \quad \sigma_{ij} = C_{ik}T_{kj} \tag{10}$$

where C_{ik}^{-1} is the inverse tensor of C_{ik} and satisfies the relation $C_{ik}^{-1}C_{kj} = \delta_{ij}$, where δ_{ij} is Kronecker's delta. Based on statistical considerations, Oda[11] derived the following proportional relation between the tensors C_{ij} and F_{ij} for a spherical assembly:

$$F_{ij} = (1/3)C_{ij} \tag{11}$$

Kaolin clay consists of platy particles. For simplicity, however, we adopt this relation as the first step of the present approach and observe the results. Equation (10) is then rewritten as:

$$T_{ij} = (1/3)F_{ik}^{-1}\sigma_{kj} \quad \text{or} \quad \sigma_{ij} = 3F_{ik}T_{kj} \tag{12}$$

The scalar 1/3 is chosen such that the modified stress tensor T_{ij} should reduce to the conventional stress tensor σ_{ij} so long as the soil is isotropic with the isotropic tensor of Eq. (4). Note, furthermore, that the modified and conventional stress tensors resulting from Eq. (12) are not symmetric, which means that $T_{ij} \neq T_{ji}$ and $\sigma_{ij} \neq \sigma_{ji}$. This leads to the characteristics of the Consserat continuum, the nonsymmetry of the stress tensor of which is related to the spinning of the unit cells (grain) of the materials (see Schaeffer[13]). In the present study, however, we consider the case of symmetric stress tensors. Thus, the stress tensors calculated by Eq. (12) are symmetrized as follows:

$$\begin{aligned} T_{ij} &= T_{ji} = (1/2)(T_{ij} + T_{ji}) \\ \sigma_{ij} &= \sigma_{ji} = (1/2)(\sigma_{ij} + \sigma_{ji}) \end{aligned} \tag{13}$$

3.3 Failure Criterion and Yield Function in terms of the Modified Stress Tensor

The modified stress was introduced based on the idea that, for granular soils, stress should be defined referring to the contact surfaces because plastic behaviors of soils occur as a result of sliding and rolling of particles at contacts. In other words, the yield function and the failure criterion should be defined in terms of the modified stress tensor, rather than the conventional stress tensor. Yield functions for isotropic soils are usually formulated in terms of the conventional stress tensor σ_{ij}. Here, it is assumed that such a yield function can be generalized by substituting T_{ij} for σ_{ij}. Ohta and Sekiguchi[14] introduces a yield function which could take into account the effects of an anisotropic initial stress condition on the plastic behavior of the materials. However, in the case of isotropic initial stress condition, the Ohta and Sekiguchi yield function coincides with the yield function of the original Cam–clay model (Schofield and Wroth[15]). In this case, the Ohta and Sekiguchi formulation of the original Cam–clay yield function can be given as:

$$f = [(\lambda - \kappa)/(1+e_0)]\ln(p/p_0) + D(q/p) = 0 \tag{14}$$

where $q = \sqrt{(3/2)s_{ij}s_{ij}}$ is proportional to the second invariant of deviatoric stress tensor $s_{ij}(=\sigma'_{ij} - p\delta_{ij})$, $p = (1/3)\sigma'_{ij}\delta_{ij}$ is the mean effective stress, $\sigma'_{ij} = \sigma_{ij} - u_w\delta_{ij}$ is the effective stress tensor, λ and κ correspond to the compression and swelling indices, respectively, D is the dilatancy coefficient representing the effect of the stress ratio increment on the volume change of clay, e_0 and p_0 are the void ratio and mean pressure at the end of consolidation, respectively. In order to account for anisotropic behaviors, all of the stress terms are replaced by their equivalences as calculated from the modified stress tensor T_{ij}. The yielding function of Eq. (14) can then be rewritten as:

$$f = [(\lambda - \kappa)/(1+e_0)]\ln(\bar{p}/\bar{p}_0) + D(\bar{q}/\bar{p}) = 0 \tag{15}$$

where $\bar{p}$, $\bar{p}_0$, and $\bar{q}$ are the equivalences in terms of modified stress; i.e., $\bar{q} = \sqrt{(3/2)S_{ij}S_{ij}}$ is proportional to the second invariant of deviatoric modified stress tensor $S_{ij}(=T'_{ij} - \bar{p}\delta_{ij})$, $\bar{p} = (1/3)T'_{ij}\delta_{ij}$ is the mean effective modified stress, and $T'_{ij} = T_{ij} - u_w\delta_{ij}$ is the effective modified stress tensor. Moreover, similar to the definition by Schofield and Wroth[15], the critical state line can be also given in terms of the modified stress as:

$$\overline{M} = \bar{q}/\bar{p} \tag{16}$$

where $\overline{M}$ is the modified critical state parameter. Note that the present approach, using fabric and modified stress tensors, for anisotropic soils can be applied for any yielding and failure criterions proposed for the isotropic soils. The present approach is said to be general in this sense. Using a parameter r (called the degree of anisotropy), we can determine a fabric tensor $F_{\alpha\beta}$ with respect to the major principal axis of anisotropy (i.e., x_α (α=1,2,3)). Referring to the global axes X_i (i =1,2,3), as discussed earlier, the fabric tensor F_{ij} is given in terms of the degree of anisotropy r and the inclination angle θ between x_1 and X_1. Note that the conventional stress tensor is calculated by $\sigma_{ij} = 3F_{ik}T_{kj}$ (Eq. (12)). Hence, even if the modified stress tensor T_{ij} is identical, the conventional stress tensor σ_{ij} differs depending on θ. As a result, the parameter $M(=q/p)$, which represents a failure line in (q,p) - space, is not constant, but rather is given as a function of the inclination angle θ. This is true even though $\overline{M}$ is constant in the modified stress space ($\bar{q}$, $\bar{p}$). Similarly, we could obtain the same result for the analysis of the stress points satisfying yielding condition. The same yielding point in terms of T_{ij} could give different equivalent yielding stress points in terms of σ_{ij} depending on θ. As the result, this modeling approach could simulate the experimental observation by Kurukulasuriya[2] that samples behave differently as being sheared at different inclination angles θ.

3.4 Constitutive Equations

Since the normality rule plays a dominant role in the classical plasticity theory, we use it in the present study. The normality rule is written as:

$$d\varepsilon_{ij}^{p} = \bar{\lambda}(\partial f / \partial\sigma_{ij}) \tag{17}$$

where $d\varepsilon_{ij}^{p}$ is the plastic strain increment tensor, and $\bar{\lambda}$ is a scalar parameter of proportionality. Using the consistency condition of $df = 0$ along with the normality rule, we can derive the following constitutive relationship:

$$d\sigma_{ij} = C_{ijkl}^{ep} d\varepsilon_{kl}$$

$$= \left[C_{ijkl}^{e} - \frac{C_{ijpq}^{e} N_{pq} N_{mn} C_{mnkl}^{e}}{N_{mn} C_{mnpq}^{e} N_{pq} - \dfrac{\partial f}{\partial \bar{p}_0} \dfrac{\partial \bar{p}_0}{\partial \varepsilon_v^p} \dfrac{\partial f}{\partial \sigma_{kk}}} \right] d\varepsilon_{kl} \tag{18}$$

where $N_{ij} = \partial f / \partial\sigma_{ij}$, C_{ijkl}^{ep} and C_{ijkl}^{e} are the elastoplastic and elastic matrixes, respectively and, $\varepsilon_v^p, \varepsilon_{ij}^p, \varepsilon_{ij}$ are the plastic volumetric strain, plastic strain, and total strain tensors. Here, $\bar{p}_0$ acts as the hardening parameter in this model with the hardening rule defined as:

$$\partial \bar{p}_0 / \partial\varepsilon_v^p = \bar{p}_0 (1 + e_0)/(\lambda - \kappa) \tag{19}$$

Details for the derivation of Eq. (18) can be found elsewhere (e.g., Desai and Siriwardane[16]). Note, however, that since the yield function f in the present model is given in terms of modified stress T_{ij}, the derivative of $\partial f / \partial\sigma_{ij}$ in Eq. (18) must be calculated as follows:

$$\partial f / \partial\sigma_{ij} = (\partial f / \partial T_{mn})(\partial T_{mn} / \partial\sigma_{ij}) \tag{20}$$

From Eq. (12), $\partial T_{ij} / \partial\sigma_{mn}$ can also be written as:

$$\partial T_{ij} / \partial\sigma_{mn} = (1/3) F_{ir}^{-1} \delta_{rm} \delta_{jn} \tag{21}$$

The constitutive equation for anisotropic soils is now completed with the inclusion of the fabric tensor. The effect of the microstructure on yielding behavior appears explicitly in the terms of F_{ij}^{-1} in Eq. (21). Note that in the calculation of Eq. (21), the fabric tensor F_{ij} is assumed to be constant, which means $\partial F_{ij} / \partial\sigma_{mn} = 0$, during a particular incremental analysis. The components of F_{ij} are only updated at the end of each loading step in a piecewise linear manner. The yield function of Eq. (15) is now a function not only of the conventional stress tensor but also of the fabric tensor. If such a yield function is used along with the normality rule (Eq. (17)), the principal axes of plastic strain increment tensor $d\varepsilon_{ij}^{p}$ are not coaxial with those of the stress tensor σ_{ij}, but rather depend on both the principal axes of σ_{ij} and F_{ij}. That is, the coaxiality in the classical plasticity model is not guaranteed in the present model. Gutierrez et al.[17], for example, pointed out that noncoaxiality is one of the most fundamental aspects of granular soils. In fact, recent experimental evidence supports the noncoaxiality for clays sheared in undrained condition (e.g., Lin and Prashant[18]). The modification of the conventional plasticity theory in Eq. (20) also leads to non-symmetry of the term $\partial f / \partial\sigma_{ij}$, which means $N_{ij} \neq N_{ji}$. However, with an isotropic elastic constitutive matrix defined as:

$$C_{ijkl}^{e} = (K - 2G/3)\delta_{ij}\delta_{kl} + G(\delta_{ik}\delta_{jl} + \delta_{il}\delta_{jk}) \tag{22}$$

The product A_{ij} of C_{ijkl}^{e} and N_{kl}, as calculated as below, retains its symmetry, which means $A_{ij} = A_{ji}$:

$$A_{ij} = C_{ijkl}^{e} N_{kl} = (K - 2G/3)\delta_{ij} N_{kk} + G(N_{ij} + N_{ji}) \tag{23}$$

where K and G in Eqs. (22) and (23) are the elastic bulk and shear modulus, respectively. Substituting Eq. (23) into Eq. (18), results in a final symmetric constitutive matrix C_{ijkl}^{ep}. Thus, all subsequent calculation procedures can be kept the same as those in the case of the conventional plasticity theory.

4. Effects of Induced Anisotropy on the Undrained Shear Strength Anisotropy

4.1 Determination of Model Parameters

The method by which to determine the parameters involved in the constitutive model is critical. Iizuka and Ohta[19] discussed in detail how to determine the parameters λ, κ and D appearing in Eq. 14. In addition, in order to define the critical state in terms of the modified stress, we newly introduce in the present study two parameters which are the degree of anisotropy at ultimate condition r_{ult} and the critical state parameter $\bar{M}$ in $(\bar{q}, \bar{p})$-stress space. Furthermore, from the value of r_{ult}, we could also obtain r_{ini} (the degree of anisotropy at the initial condition) using the simple relationship described in the previous part of the paper. Here, we focus on the determination of r_{ult} and $\bar{M}$ referring to the experimental data of normally consolidated

Kaolin clay. Let us choose a modified stress point $(\overline{q}, \overline{p})$ located on the critical state line, namely, $\overline{q}/\overline{p} = \overline{M}$. Assuming further that T_{11}, T_{22} and T_{33} $(=T_{11})$ are the principal stresses with a maximum principal value equal to T_{22}, we can express the critical parameter $\overline{M}$ as:

$$\overline{M} = \overline{q}/\overline{p} = 3(T_{22} - T_{11})/(T_{22} + 2T_{11}) \tag{24}$$

If the minimum stress T_{33} $(=T_{11})$ is set to unity, the modified stress tensor T_{ij}^F on the critical state line can be written in terms of $\overline{M}$ as:

$$\begin{aligned} T_{ij}^F &= (T_{11}, T_{22}, T_{33}, T_{12}, T_{23}, T_{13}) \\ &= \left(1, (3+2\overline{M})/(3-\overline{M}), 1, 0, 0, 0\right) \text{ (kPa)} \end{aligned} \tag{25}$$

It is of particular importance to know that the stress of Eq. (25) is representative for many conventional stresses σ_{ij}^F at failure corresponding to various sets of r_{ult} and θ. Since the fabric tensor F_{ij} is given in terms of r_{ult} and θ, the stress σ_{ij}^F at failure corresponding to T_{ij}^F can be calculated using the equation $\sigma_{ij}^F = 3F_{ik}T_{kj}^F$. By changing the value of $\overline{M}$ in Eq. (25), we can obtain various σ_{ij}^F, and the corresponding values of q^F and p^F at failure. M is then calculated as q^F/p^F for any set of r_{ult} and θ. In this way, we obtain an entire data set of $(r_{ult}, M, \overline{M})$ for a given inclination angle θ. Note that the relation among r_{ult}, M and $\overline{M}$ is independent of the choice of T_{ij}^F (Eq. (25)). On one hand, M can also be experimentally determined using q and p at failure for any selected values of θ by using the experimental data conducted by Kurukulasuriya[2]. Hereinafter, two values of M experimentally determined at $\theta = 30^\circ$ and $\theta = 90^\circ$ are denoted as $M^t_{\theta=30^\circ}$ and $M^t_{\theta=90^\circ}$, respectively. From the previously calculated data set of $(r_{ult}, M, \overline{M})$ for $\theta = 30^\circ$ and $\theta = 90^\circ$, we can obtain different combinations of $(r_{ult}, \overline{M})$ corresponding to $M^t_{\theta=30^\circ}$ and $M^t_{\theta=90^\circ}$. These values of $(r_{ult}, \overline{M})$ are separately plotted in Fig. 5 for $\theta = 30^\circ$ and $\theta = 90^\circ$. In each case of $\theta = 30^\circ$ and $\theta = 90^\circ$, a straight line is used to fit the data points of $(r_{ult}, \overline{M})$.

Any point on these two lines represent different combinations of $(r_{ult}, \overline{M})$ which yield the same value of M^t_θ. Since $\overline{M}$ is uniquely defined irrespective of θ, its value and the corresponding value of r_{ult} can be determined at the intersection of the two lines corresponding to $\theta = 30^\circ$ and $\theta = 90^\circ$ in Fig. 5. Consequently, their values are determined as $\overline{M} = 0.935$ and $r_{ult} = 1.06$. (The two values of M^t_θ at $\theta = 30^\circ$ and $\theta = 90^\circ$ were specially chosen to determine r_{ult} and $\overline{M}$ because the effects of the modified stress on the ultimate parameter in this model lead to the characteristics that M^t_θ must increase with increasing θ (see Minh et al,[9]). Such an increase is experimentally observed only in the limited range of θ from 30° to 90°. The decrease of undrained shear strength with θ from 0° to 30° in Fig. 2, as will be described later, is due only to the effects of microstructural anisotropy on the plastic deformation of Kaolin clay.). It should be noted that since r is calculated using the measured stress values, the degree of anisotropy is obtained by using a phenomenological method in this study.

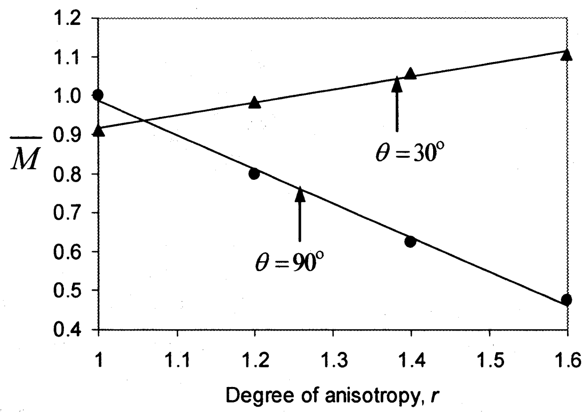

Fig. 5 Parameter determination (Kurukulasuriya[2])

Other parameters used in the yield function were calculated according to the method suggested by Iizuka and Ohta[19], as follows:

$$\begin{aligned} \Lambda &= \overline{M}/1.75 \\ \lambda &= 0.015 + 0.007PL \\ D &= \lambda\Lambda / \left[\overline{M}(1+e_0)\right] \end{aligned} \tag{26}$$

where $\Lambda = (1 - \kappa/\lambda)$ is a parameter related to the irreversible volume change, as shown by the last equation of Eq. (26), and PL the plasticity index, which is equal to 51.2% for Kaolin clay. Generally speaking, clay might be anisotropic in the elastic response. However, for simplicity, Young's modulus E and the Poisson ratio ν were determined based on the assumption of isotropy, as summarized in Table 1 for normally consolidated Kaolin clay.

Table 1 Input parameters for numerical modeling

$\overline{M}$	r_{ult}	Λ	λ	D	ν	E(kPa)
0.935	1.060	0.534	0.373	0.085	0.373	8000

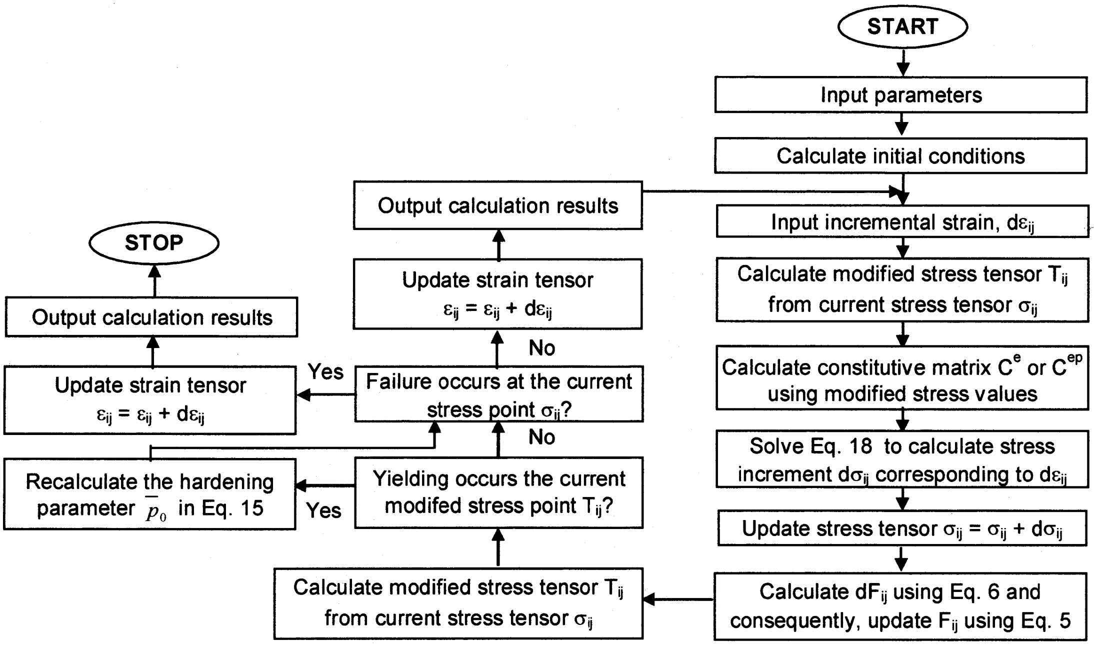

Fig. 6 Flow chart of the program used for numerical modeling of undrained shear strength anisotropy

4.2 Modeling Results on the Effects of Induced Anisotropy on the Undrained Shear Strength Anisotropy

Based on the plasticity theory, a program code was written to calculate numerically the integration of the constitutive equation in Eq. (18) so as we could obtain the stress and strain behaviors of the soil samples sheared under the undrained condition. With the incorporation of the fabric and modified stress tensors into the conventional plasticity theory, the main target of the written program is to simulate the undrained shear strength anisotropy of Kaolin clay. Figure 6 shows a flow chart of the main steps of the program. A numerical analysis was carried out by means of controlling strain increments. The requirement of undrained plane strain was implemented such that $d\varepsilon_{11} + d\varepsilon_{22} = 0$ and $d\varepsilon_{33} = 0$.

The elastic matrix C^{e}_{ijkl} and the elastoplastic matrix C^{ep}_{ijkl} were first calculated at the current modified stress point, and then Eq. (18) was solved to obtain the corresponding stress increments. The modified stress was calculated twice in a complete running loop of Fig. 6, namely, to calculate the matrixes C^{ep}_{ijkl}, and to check whether the yielding condition of Eq. (15) was satisfied at the current state. Note, however, that the failure condition was checked in terms of conventional stress in the same manner as the common approach of constitutive modeling. Here, M was computed from the value of $\overline{M}$ and $(F_{ij})_{ult}$ at the beginning of the first calculation step and was then used throughout the simulation process. It should be noted that the values of r_{ini} and r_{ult}, which also define $(F_{ij})_{ini}$ and $(F_{ij})_{ult}$, are calculated from the experimental data based on the assumption of transverse anisotropy in Eq. (2). On the other hand, the fabric tensor at the last loading step, $(F_{ij})^{F}$, may not be transverse anisotropic. Its value depends on both the initial fabric tensor $(F_{ij})_{ini}$ and the stress path, which controls the term ds_{ij} of the evolution rule in Eq. (6). As the result, $(F_{ij})^{F}$ should not be necessarily the same as $(F_{ij})_{ult}$, however, according to the evolution rule in Eq. (8), the second deviatoric invariant of $(F_{ij})^{F}$ will not exceed the value of $(\sqrt{J^{F}_{2D}})_{ult}$ calculated from $(F_{ij})_{ult}$. In other words, at the ultimate condition of the fabric tensor, the components of the fabric tensors need not be uniquely defined but their second deviatoric invariants are uniquely defined as being equal to $(\sqrt{J^{F}_{2D}})_{ult}$ irrespective of the stress path leading to failure.

Figure 7 shows the experimental and simulated results of the undrained shear strength anisotropy of normally consolidated Kaolin clay, which also includes the simulated result of inherent anisotropy from Minh et al.[9] for comparison. It is shown in Fig. 7 that the modeling of inherent anisotropy could only simulate a monotonic increase of undrained shear strength with θ and, hence, fail to agree with the experimental data for θ ranging from 0° to 30°. The modeling of induced anisotropy, on the other hand, could capture well the full range of undrained shear strength anisotropic behavior of Kaolin clay observed by Kurukulasuriya[2].

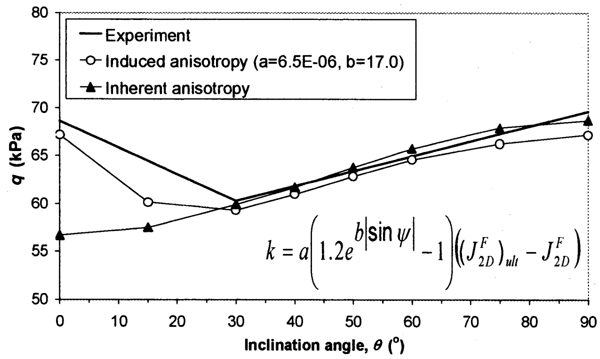

Fig. 7 Experimental and simulated results on the undrained shear strength anisotropy of NC Kaolin clay

By conducting parametric studies, we could obtain the following values of $a = 6.5\times10^{-6}$ and $b = 17.0$ for the evolution parameters in Eq. (8). With the parameter b is set as much as 17.0, k changes very rapidly within $60^\circ \le \psi \le 90^\circ$, so that the induced anisotropy develops very quickly parallel to the compression direction X_2 (see Fig. 3). Note that ψ equals ($90^\circ - \theta$) in an early stage of deformation at least, hence microstructure changes significantly if θ is within 0° to 30°. Let us consider the case of $\theta = 0^\circ$ as a typical example. Initially, the major principal axis x_1 of the initial fabric tensor F_{ij} is parallel to the global axis X_1. The major principal axis of ds_{ij} is parallel to X_2 since the soil sample is compressed parallel to the X_2 axis. Accordingly, ψ equals 90° so that the induced anisotropy develops quickly in the direction of X_2. As a result, the major principal axis x_1 of the (induced) fabric tensor is rotated so quickly that it becomes parallel to the axis X_2 (not the axis X_1 at the beginning). In other words, the induced fabric looks similar to the case of $\theta = 90^\circ$. This explains for the observation that the undrained shear strength in the case of $\theta = 0^\circ$ is drastically improved until it reaches the shear strength in the case of $\theta = 90^\circ$.

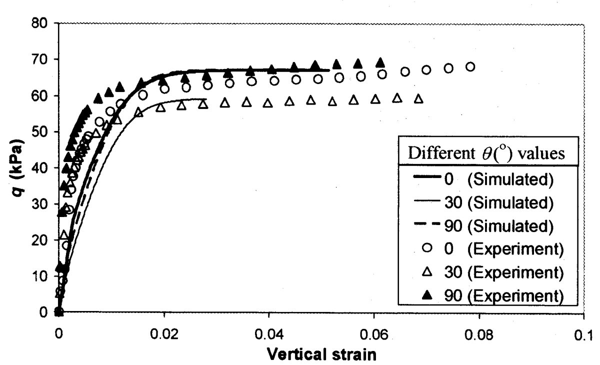

Fig. 8 Experimental and modeling stress–strain curves with different θ(°) values

In Fig. 8, the stress–strain curves calculated numerically using $(a,b) = (6.5\times10^{-6}, 17.0)$ are compared with the results obtained from plane strain tests of normally consolidated Kaolin clay. The stress–strain curves in the cases of $\theta = 0^\circ$ and $\theta = 90^\circ$ possess higher shear strength and stiffness in comparison with the case of $\theta = 30^\circ$. The constitutive model, however, predicts smaller failure strain as well as smaller initial stiffness, as compared with the experimental results. Figure 9, on the other hand, shows the simulated and experimental stress paths. Although there are discrepancies regarding the magnitude of the experimental and simulated results in Fig. 8 and Fig. 9, there exists similar tendency between the experimental data and simulation results for the shifting of the stress paths as well as the stress-strain curves with different θ values. For example, in the case of $\theta = 0^\circ$ in Fig. 9, both the experimental and simulated stress paths move along a vertical line in the beginning of shearing process, which leads to significant higher shear strengths in comparison with the stress path of $\theta = 30^\circ$. This is consistent with the higher stiffness observed in Fig. 8. This characteristic can be considered as a merit of the proposed constitutive model as, for example, if the original Cam clay model is applied in the simulation then only one unique stress path can be produced for the same experimental data set irrespective of the θ value. The prediction of the deformation characteristics of the sample, on the other hand, can be improved by employing a more complicated dilatancy relationship in the constitutive model framework. This is, however, beyond the scope of this study at the present stage because the study is firstly concentrated on setting up a continuum modeling approach for the microstructural evolution. In doing so, it is an attempt to start first with a rather simple and well-established theoretical framework like the original Cam clay model.

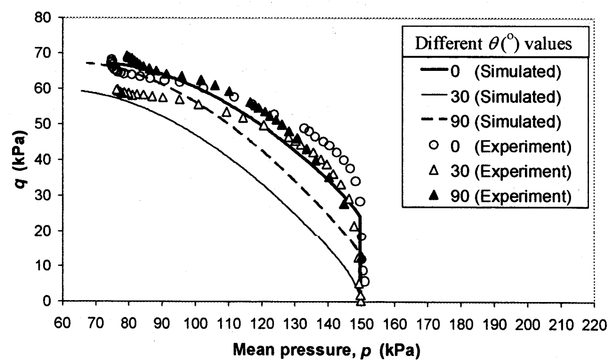

Fig. 9 Experimental and modeling stress paths with different θ(°) values

Since the plastic deformation is closely related to the development of excess pore water pressure in the undrained condition, the higher undrained shear strength obtained at $\theta = 0^\circ$ could be mainly due to the anisotropy in terms of excess pore water pressure development. As θ gaining higher values from 30° to 90°, the evolution rule defined in Eq. (8) leads to slower evolution of the fabric tensor, the effects of the induced anisotropy on the plastic deformation hence becomes less dominant in this range. Consequently, the effects of induced anisotropy on the shear strength parameter now become the controlling factor. This could explain for the tendency that, with θ from 30° to 90°, undrained shear strength increases monotonically with θ, which is similar to the relationship between the critical parameter M and θ.

5. Discussion and Concluding Remarks

The microstructure of soils is, in general, anisotropic in both the "inherent" and "induced" senses, as described by Casagrande and Carillo[1]. Therefore, anisotropic responses are obtained for both strength and plastic deformation. Undrained shear strength of clayey soils, for example, changes greatly depending on the inclination angle θ of the loading direction with respect to the consolidation plane. In the present study, a tensorial quantity (called the fabric tensor) is incorporated into the framework of the classical plasticity theory to simulate the microstructure of Kaolin clay. Furthermore, the effects of both inherent and induced anisotropies can be taken into account with the introduction of an evolution rule of the fabric tensor during the shearing process as well as its stationary values at the initial and ultimate conditions. The results of numerical simulations can be summarized as follows. 1) The anisotropy in the undrained shear strength of Kaolin clay is caused by both the anisotropy in terms of shear strength parameters and the anisotropy plastic response, which leads to anisotropy in excess pore water pressure development. 2) By taking the evolution of the fabric tensor (induced anisotropy) into account, the proposed model can simulate well the variation of undrained shear strength with θ observed from the plane strain experiments by Kurukulasuriya[2] for normally consolidated Kaolin clay. 3) The incorporation of the fabric tensor into the yield function in this model naturally leads to noncoaxiality between the plastic strain increment tensor and the stress tensor, which has been confirmed experimentally (e.g., Lin and Prashant[18]) for Kaolin clay sheared under the undrained condition. 4) The proposed approach may be used to incorporate the results of discrete studies into the continuum constitutive modeling of soils.

References

1) Casagrande, A. and Carillo, N., Shear failure of anisotropic materials, *Proc. Boston Soc. Civ. Engrs.*, 31, pp. 74–87, 1944.
2) Kurukulasuriya, L.C., *Undrained shear strength of an overconsolidated clay and its effects on the bearing capacity of strip footing,* Doctoral Dissertation, Saitama University, Japan, 1998.
3) Kazama, H., *Study on micro-structure of clayey soils and their effects on their consolidation and shear behaviors*, Doctoral Dissertation, Saitama University, Japan, 1996.
4) Oda, M., The mechanism of fabric changes during compressional deformation of sand, *Soils and Foundations*, 12 (2), pp. 1–18, 1972.
5) Satake, M., Fabric tensor in granular materials, *Proc. IUTAM Conference on Deformation and Failure of Granular Materials*, Balkema, Rotterdam, pp. 63-68, 1982.
6) Oda, M., Nemat-Nasser, S. and Mehrabadi, M.M., A statistical study of fabric in a random assembly of spherical granules, *Int. J. for Num. & Ana. Meth. in Geomech.*, 6, pp. 77-94, 1982.
7) Duncan, J.M. and Seed, H.B., Anisotropy and stress reorientation in clay, *J. of SMFE Div.*, ASCE, 92 (SM5), pp. 21–50, 1966.
8) Duncan, J.M. and Seed, H.B., Strength variation along failure surfaces in clay, *J. of SMFE Div.*, ASCE, 92 (SM6), pp. 81–104, 1966.
9) Minh, N.H., Oda, M., Suzuki, K. and Kurukulasuriya, L.C., Modeling of inherent anisotropy to simulate undrained shear strength variation of Kaolin clay, Submitted to the *J. of Engineering Mechanics*, ASCE, 2008.
10) Ohta, H. and Nishihara, A., Anisotropy of undrained shear strength of clays under axi-symmetric loading conditions, *Soils and Foundations*, 25(2), pp. 73–86, 1985.
11) Oda, M., Inherent and induced anisotropy in plasticity theory of granular soils, *Mechanics of Materials*, 16, pp. 35–45, 1993.
12) Tobita, Y., Contact tensor in constitutive model for granular materials, *Proc. US-Japan Seminar on Micromechanics of Granular Materials*, Jenkins and Satake, eds., Elsevier, Amsterdam, pp. 263-270, 1988.
13) Schaeffer, H., Das Cosserat–Kontinuum, *ZAMM*, 47, pp. 485–498, 1967.
14) Ohta, H. and Sekiguchi, H., Constitutive equations considering anisotropy and stress orientation in clay, *Proc. 3rd Int. conf. on Numerical Method in Geomechanics*, Aachen, pp. 475–484, 1979.
15) Schofield, A. and Wroth, P., *Critical State Soil Mechanics*, McGraw–Hill, London, 1968.
16) Desai, C.S. and Siriwardane, H.J., *Constitutive laws for engineering materials with emphasis on geologic materials,* Prentice–Hall, Inc., New Jersey, 1984.
17) Gutierrez, M., Ishihara, K. and Towhata, I., Noncoaxiality and stress dilatancy relations for granular materials, *Computer method and advanced in geomechanics*, G. Beer, J.R. Bookeer and J.P. Carter, eds., Balkema, Rotterdam, pp. 625–630, 1991.
18) Lin, H. and Prashant, A., Single hardening elasto–plastic model for Kaolin clay with loading–history–dependent plastic potential function., *Int. J. of Geomechanics*, ASCE, 6 (1), pp. 55–63, 2006.
19) Iizuka, A. and Ohta, H., A determination procedure of input parameters in elasto–viscoplastic finite element analysis, *Soils and Foundations*, 27 (3), pp. 71–87, 1987.

(Received: April 14, 2008)